HELDA
HELSINGIN YLIOPISTO
HELSINGFORS UNIVERSITET
UNIVERSITY OF HELSINKI

UNIVERSITY OF HELSINKI

https://helda.helsinki.fi

Automated SEA ICE Classification Over the Baltic SEA using Multiparametric Features of Tandem-X Insar Images

Marbouti, Marjan

IEEE
2018-11-05

Marbouti , M , Antropov , O , Eriksson , P , Praks , J , Arabzadeh , V , Rinne , E & Leppäranta , M 2018 , Automated SEA ICE Classification Over the Baltic SEA using Multiparametric Features of Tandem-X Insar Images . in 2018 IEEE International Geoscience and Remote Sensing Symposium : Observing, Understanding And Forecasting The Dynamics Of Our Planet . IEEE International Symposium on Geoscience and Remote Sensing IGARSS , IEEE , pp. 7328-7331 , 38th IEEE International Geoscience and Remote Sensing Symposium (IGARSS) , Valencia , Spain , 22/07/2018 . https://doi.org/10.1109/IGARSS.2018.8518996

http://hdl.handle.net/10138/311622
https://doi.org/10.1109/IGARSS.2018.8518996

acceptedVersion

Downloaded from Helda, University of Helsinki institutional repository.

This is an electronic reprint of the original article.

This reprint may differ from the original in pagination and typographic detail.

Please cite the original version.

AUTOMATED SEA ICE CLASSIFICATION OVER THE BALTIC SEA USING MULTIPARAMETRIC FEATURES OF TANDEM-X INSAR IMAGES

Marjan Marbouti [a], Oleg Antropov [b], Patrick Eriksson [c], Jaan Praks [b], Vahid Arabzadeh [d], Eero Rinne [c], Matti Leppäranta [a]

[a] Institute for Atmospheric and Earth System Research / Physics, Faculty of Science, University of Helsinki, Finland;
[b] Department of Electronics and Nano engineering, Aalto University, P.O. Box 13000, 00076, Finland;
[c] Finnish Meteorological Institute, Marine Research, Erik Palméninaukio 1, 00560, Helsinki, Finland;
[d] Aalto University, School of Science, New Energy Technologies Group, Aalto, Espoo, Finland;

ABSTRACT

In this study, bistatic interferometric Synthetic Aperture Radar (InSAR) data acquired by the TanDEM-X mission were used for automated classification of sea ice over the Baltic Sea, in the Bothnic Bay. A scene acquired in March of 2012 was used in the study. Backscatter-intensity, coherence-magnitude and InSAR-phase, as well as their different combinations, were used as informative features in several classification approaches. In order to achieve the best discrimination between open water and several sea ice types (new ice, thin smooth ice, close ice, very close ice, ridged ice, heavily ridged ice and ship-track), Random Forests (RF) and Maximum likelihood (ML) classifiers were employed. The best overall accuracies were achieved using combination of backscatter-intensity & InSAR-phase and backscatter-intensity & coherence-magnitude, and were 76.86% and 75.81% with RF and ML classifiers, respectively. Overall, the combination of backscatter-intensity & InSAR-phase with RF classifier was suggested due to the highest overall accuracy (OA) and smaller computing time in comparison to ML. In contrast to several earlier studies, we were able to discriminate water and the thin smooth ice.

Index Terms— Remote sensing, sea ice classification, random forests, Maximum likelihood, TanDEM-X.

1. INTRODUCTION

Synthetic Aperture Radar (SAR) data were used to monitor ice covered maritime regions for more than three decades. SAR data are independent of cloud coverage, and sunlight conditions [1]. SAR satellites are able to cover almost whole Earth within short periods while airborne and shipborne data have limitations regarding coverage and weather condition [2]. Sea ice classification is a critical topic that was investigated for many years. Majority of ice classification studies were done with C-band SAR data [3-5], and only few studies were done with X-band data. The reason is that spaceborne X-band SAR data were not readily available until recently [1,6].

In the Baltic Sea, winter navigation is the main motivation for ice classification research. Finnish Meteorological Institute (FMI) provide daily ice charts for sea ice condition. FMI uses SAR satellites, especially operating at C-band, e.g., Radar Satellite-2 (RADARSAT-2) and, Sentinel-1 [7]. These sensors have good resolution, although extracting more information about detailed ice properties, ice ridges and heavily deformed ice requires sensors with higher resolution available from such missions as TanDEM-X. Another advantage of X-band SAR over C-band is higher sensitivity toward surface conditions [1,8]. Presently, the FMI service uses trained experts for sea ice classification and ice chart production. However, this method is time consuming and expensive. Furthermore, the same SAR data interpreted by different experts can, and often does, lead to somewhat different end results. Automatic sea ice classification has potential to solve these problems to considerable extent. To date, there are some demonstrations of automated ice classification using backscatter-intensity data [5,7]. Previous works [1,9,10] have concluded that using only the backscatter-intensity is not sufficient to automatically classify ice types due to similar backscatter-intensity values between classes. Studies focusing on interferometric SAR (InSAR) properties of sea ice [11,12,13] have demonstrated that coherence-magnitude data provides auxiliary information about sea ice characteristics and ice dynamics. In this study, we investigate the effect of using various SAR/InSAR features (backscatter-intensity, coherence-magnitude and InSAR-phase) and their combinations for improving automatic sea ice classification at X-band, and try to establish an optimal workflow for automatic classification using data from the first spaceborne bistatic InSAR mission, TanDEM-X. To date, there was only one study [6] focusing on sea ice type classification from TanDEM-X data using the mean backscatter-intensity and coherence-magnitude values. Their method was applied over few types of sea ice such as fast ice, thin smooth ice, pancake ice and water. In this study,

we expand the scope and apply two state-of-the-art classification algorithms, Random Forests (RF) and Maximum likelihood (ML) on more types of sea ice (new ice, thin smooth ice, close ice, very close ice, ridged ice, heavily ridged ice and ship-track) by using more features and their combinations, and compare RF and ML classification algorithms. The objectives of the current study are:
(i) To determine optimal combination of SAR/InSAR image features and their relative performance, for discriminating different sea ice classes using X-band InSAR data;
(ii) To determine the optimal classification approach.

2. MATERIALS AND METHODS

2.1. Test site and InSAR

The TanDEM-X SAR data were acquired near the Hailuoto Island in the north of the Baltic Sea on 30th March 2012. TanDEM-X coregistrated Single Look Slant Range Complex (CoSSC) product was used in the current study for ice type characterization. The scene included backscatter-intensity, coherence-magnitude and InSAR-phase were in stripmap mode, had bistatic operational mode and polarization HH were available. As high incidence angle imagery were suggested by Laanemae [6] for water/ice classification, the highest incidence available angle, 43.417 degrees was used in this study. A 7×7 boxcar filter was applied over SAR features, then the land area was removed by applying land masking. Image stretching was applied over image features for dynamic range equalization. This procedure re-distributes values of an image features over a wider or narrower range of values in output features.

2.2. Reference classification map

In the Baltic Sea, ice charts are prepared by the FMI experts. The ice charts provide a daily source of information on the ice conditions. The charts are based on visual interpretation of SAR imagery as the principal source of information [7]. Experts also use visible and thermal infrared imagery from Moderate Resolution Imaging Spectroradiometer (MODIS), in-situ observations, sea ice reports from icebreakers, and sea ice models in the production of the ice charts. TanDEM-X features are backscatter-intensity, coherence- magnitude and InSAR-phase. These features have not been used in ice chart preparation. These features help experts to make more accurate ice charts and also distinguish ice ridges, heavily deformed ice and new ice formation. In this study, TanDEM-X features were used by sea ice expert in producing the reference map (Figure 1).

2.3. Training and classifications (RF and ML)

To improve classification performance, careful selection of training data is crucial [14]. In this study, the training plots were selected from reference map made by sea ice expert. Our reference map included eight types of sea ice (although one of them is water). In overall, six rectangular plots were selected per any class (three plots for training and three others for validation). Thus, a total of 24 (8*3=24) rectangular training plots were used. As our image features included huge number of pixels, it was necessary to choose a robust, effective classifier for sea ice classification. RF classifier has proven its power in handling classification with a big data of high dimensional feature spaces [15]. There are several free software tools offering RF implementation. In this study, Orfeo ToolBox (OTB) was used. Number of trees in the forest and the maximum depth of the tree were 100 and 5, respectively. Another popular supervised classification approach routinely used in remote sensing applications is Maximum Likelihod (ML). Implementation provided by the Sentinel Application Platform (SNAP) of ESA was used to perform the supervised ML pixel-based image classification.

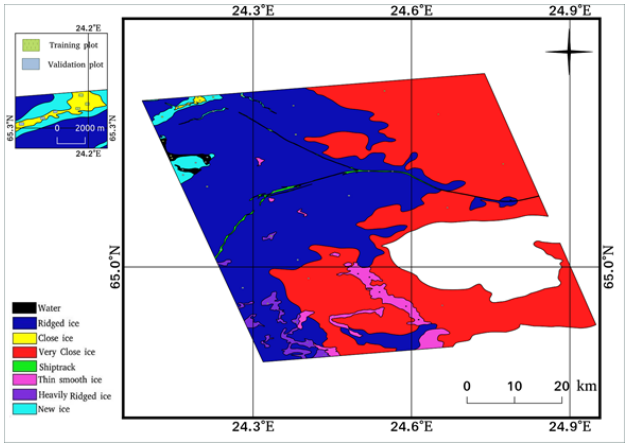

Fig. 1. Reference classification map produced by sea ice expert for March 20, 2012. Six plots were depicted from any classes (three training plots and three validation plots). Close ice class was enlarged in upper left corner of image, and also training and validation plots are shown on it.

2.4. Using stratified sampling design for validation

Accuracy assessment methodology includes three components, the response design, sampling design, and analysis. As the intention is to present results per each class in equally, the stratified sampling method was applied for validation. Three rectangular plots per every class were chosen randomly. Also, the majority voting in a ball shaped neighborhood with radius three was applied for filtering the classification results.

3. RESULTS

Based on 14 classification experiments, confusion matrices were calculated for seven types of single and combinations of features including backscatter-intensity, coherence-magnitude, InSAR-phase, backscatter-intensity & coherence-magnitude, backscatter Intensity & InSAR-phase, coherence-magnitude & InSAR-phase, and backscatter-intensity & coherence-magnitude & InSAR phase features in RF and ML classifiers. The best overall accuracies (OAs) were achieved using combination of backscatter-intensity & InSAR-phase

and backscatter-intensity & coherence-magnitude, and were 76.86% and 75.81% with RF and ML classifiers, respectively. We summarized the user accuracies (UAs) of all input features and their combinations in Tables 1 and 2 for RF and ML classifiers. Figure 2 shows produced classification map of sea ice classes with the highest overall accuracy.

Table 1: UA in RF classifier for each open water and sea ice classes, single features and their combinations (B = Backscatter-intensity, C = Coherence-magnitude, I= InSAR-phase).

RF(UA)	B	C	I	B-C	B-I	C-I	B-C-I
Open-water	100	100	100	100	100	100	100
Ridged-ice	63.61	24.3	0	39.88	0	0.19	0
Close-ice	8.93	80.29	36.56	83.88	95.5	93.91	96.13
Very-close-ice	96.9	56.02	0	96.84	94.38	0	92.74
Ship-track	12.25	19.65	68.83	1.15	68.83	63.89	3.28
Thin-smooth-ice	70.4	95.62	99.29	80.21	91.76	100	92.99
Heavily-ridged-ice	49.13	4.54	0	61.03	100	97.4	72.07
New-ice	100	100	100	100	100	100	100

Table 2: UA in ML classifier for each water and sea ice classes, single features and their combinations (B = Backscatter-intensity, C = Coherence-magnitude, I= InSAR-phase).

ML(UA)	B	C	I	B-C	B-I	C-I	B-C-I
Open-water	100	100	100	100	100	100	100
Ridged-ice	82.25	68.89	0	80.4	0.57	0	3.05
Close-ice	18.06	81.74	74.27	88.21	95.31	95.5	97.02
Very-close-ice	76.37	41.98	0	36.95	92.51	4.91	13.09
Ship-track	12.91	68.66	68.83	45.8	63.32	47.28	44.49
Thin-smooth-ice	55.69	46.23	73.55	69	85.46	100	93.87
Heavily-ridged-ice	45.23	0	0	25.54	100	93.93	100
New-ice	100	100	100	100	100	100	100

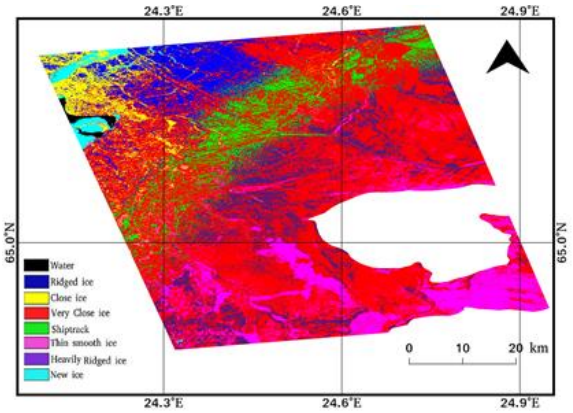

Fig. 2. Final RF classification map (backscatter-intensity & InSAR-phase combination with RF classification).

4. DISCUSSION

4.1. Relative performance of different SAR features and their combinations in RF and ML classifiers

Accuracy assessment was performed for the different combinations of features. OAs for produced maps in RF-experiments indicated that combinations of backscatter-intensity & InSAR-phase combination had the best OA by amount 76.86%, although backscatter-intensity & coherence-magnitude and coherence-magnitude & InSAR-phase combinations were listed in second and third orders by 70.11% and 67.53% respectively. The computation time for RF classification step was almost two minutes per any image feature and it increased a bit by using two or three features combination. OAs in ML-experiments indicated that backscatter-intensity & coherence-magnitude and backscatter-intensity & InSAR-phase combinations had the highest OAs by amounts 75.81% and 75.63% respectively. Coherence-magnitude feature had the third highest OA with 73.52% in ML-experiments. The computation time for ML classification was more than three minutes per any image feature and it increased a bit by using two or three features combination.

Based on Tables 1 & 2, open water and new ice areas were very well classified in classification experiments, with 100% UA. InSAR-phase feature and its combination by other features were not able to classify ridged ice (almost 0%). UAs of close ice were better when features were combined. Heavily ridged ice was not classified by separate coherence-magnitude and InSAR-phase features in classification experiments although it was well classified by using backscatter-intensity & InSAR-phase and backscatter-intensity & coherence-magnitude & InSAR-phase combinations in ML experiments and backscatter-intensity & InSAR-phase combination in RF experiments. Unlike heavily ridged ice, thin smooth ice was almost completely classified by using separated coherence-magnitude and InSAR-phase features in RF classifier; but their UAs in ML-experiments were much lower than RF-experiments. Thin smooth ice was extremely well (up to 100% UA) classified using coherence-magnitude & InSAR-phase combination in classification experiments. The ship-track did not have high UAs in RF and ML classification experiments. Our algorithms were partly successful in detecting the ship-track feature, but the properties of the type of brash ice can be found also in naturally formed ice regimes clearly representing something else than ship-tracks. Therefore we suggest other methods for discriminating ship tracks from the rest of the ice, e.g. by segmentation and shape feature detection [16]. Backscatter-intensity was a robust feature in very close ice classification. Very close ice had the highest UA in RF by using only backscatter-intensity feature, it was also high in ML classifier as well, although the highest one in ML experiments was backscatter-intensity & InSAR-phase combination. Based on the discussion, we can conclude that backscatter-intensity &

InSAR-phase and backscatter-intensity & coherence-magnitude combinations in RF and ML classification experiments were the best choices respectively. However, our recommendation is using RF classification approach based on combined backscatter-intensity & InSAR-phase due to following reasons: 1) the highest OA among all RF and ML experiments, 2) the processing and run time was quicker compared to ML.

4.2. Comparison with previous studies

Laanemae et al. [6] classified water and sea ice types over coastal sea in the Gulf of Riga based on the threshold values of the backscatter-intensity and coherence-magnitude properties for fast ice, thin smooth ice, pancake ice and water. Calculations were performed by using pair HH-Monostatic-VV-Monostatic data for coherence-magnitude calculation and HH-Monostatic data for intensity calculations. Figure 1 in [6] and previous studies [17] show that discrimination between water and thin smooth was very difficult but in our study, water and thin smooth ice were well discriminated due to using bistatic Tandem-X imaging mode. Temporal baseline of bistatic Tandem-X imaging mode is zero and wind speed would not be able to make decorrelation.

5. CONCLUSION

In this study, different features (such as backscatter-intensity, coherence-magnitude and InSAR-phase) and their combinations (backscatter-intensity & coherence-magnitude, backscatter Intensity & InSAR-phase, coherence-magnitude & InSAR-phase, and backscatter-intensity & coherence-magnitude & InSAR phase) were used for discriminating different sea ice classes (ridged ice, close ice, very close ice, ship-track, thin smooth ice, heavily ridged ice and new ice) and open water. Two supervised classifiers, RF and ML, were applied. The best results were provided by combined backscatter-intensity & InSAR-phase (OA of 76.86% when RF was applied) and combined backscatter-intensity & coherence-magnitude (OA of 75.81% with ML approach). RF algorithm turned out to be a preferable algorithm due to short runtime, higher overall and user accuracies. This study is a first approach to use backscatter-intensity, coherence-magnitude and InSAR-phase features simultaneously in sea ice classification. Also comparison RF and ML classifiers over feature combinations is another novelty of this paper. Discrimination of water and thin smooth ice was difficult in previous studies [6, 17] although this problem was solved in our study due to using bistatic imaging mode. Our further research experiments over this test site are described in [18].

6. REFERENCES

[1] R. Ressel, A. Frost, and S. Lehner, "A Neural Network-Based Classification for Sea Ice Types on X-Band SAR Images," *IEEE J. Sel. Topics Appl. Earth Obs. Remote Sens*., vol. 8, no. 7, pp. 3672-3680, July 2015.

[2] R. Ressel, S. Singha, "Comparing near coincident space borne C and X band fully polarmetric SAR data for Arctic Sea Ice classification," *Remote Sens*., vol. 8 , no. 3 , 198, 2016.

[3] W. Dierking and C. Wesche, "C-Band radar polarimetry–Useful for detection of icebergs in sea ice?" *IEEE Trans. Geosci. Remote Sens.*, vol. 52, no. 1, pp. 25–37, Jan. 2014.

[4] L.-K. Soh and C. Tsatsoulis, "Texture analysis of SAR sea ice imagery using gray level co-occurrence matrices," *IEEE Trans. Geosci. Remote Sens.*, vol. 37, no. 2, pp. 780–795, Mar. 1999.

[5] L.-K. Soh, C. Tsatsoulis, C. Bertoia, "ARKTOS: An intelligent system for SAR sea ice image classification," *IEEE Trans. Geosci. Remote Sens.*, vol. 42, no. 1, pp. 229–248, Jan. 2004.

[6] K. Laanemaee, R. Uiboupin, S. Rikka, "Sea Ice Type Classification in the Baltic Sea from TanDEM-X Imagery," *EUSAR 2016: 11th European Conf. Synthetic Aperture Radar*, Proceedings of, VDE, Hamburg, Germany, Sept. 2016.

[7] A. Gegiuc, M. Similä, J. Karvonen, M. Lensu, M. Mäkynen, and J. Vainio, "Estimation of Degree of Sea Ice Ridging Based on Dual-Polarized C-band SAR Data," *The Cryosphere*, in review, 2017.

[8] W. Dierking, "Sea ice monitoring by synthetic aperture radar," *Oceanography*, vol. 26, no. 2, pp. 100–111, 2013.

[9] M. Mäkynen, M. Hallikainen, "Investigation of C-and X-band intensitysignatures of Baltic Sea ice," *Int. J. Remote. Sens*., vol. 25, no. 11, pp.2061-2086, 2004.

[10] W. Dierking, "Mapping of Different Sea Ice Regimes Using Images From Sentinel-1 and ALOS Synthetic Aperture Radar," *IEEE Trans. Geosci. Remote Sens.*, vol. 48, no. 3, pp.1045-1058, 2010.

[11] P. Dammert, M. Leppäranta, J. Askne, "SAR interferometry over Baltic Sea ice," *Int. J. Remote. Sens*., vol. 19, no. 16, pp. 3016-3037, 1998.

[12] A. Berg, P. Dammert, L. Eriksson, "X-Band interferometric SAR observations of Baltic fast ice," *IEEE Trans. Geosci. Remote Sens.*, vol. 53, no. 3, pp.1248-1256, 2015.

[13] M. Marbouti, J. Praks, O. Antropov, E. Rinne, M. Leppäranta, "A study of landfast ice with Sentinel-1 repeat-pass interferometry over the Baltic Sea," *Remote Sens.*, vol. 9 , no. 8 , 833, 2017.

[14] O. Antropov, Y. Rauste, H. Astola, J. Praks, T. Häme, and M.T. Hallikainen, "Land cover and soil type mapping from spaceborne PolSAR data at L-Band with probabilistic neural network," *IEEE Trans. Geosci. Remote Sens.*, vol. 25, no. 9, pp.5226-5270, 2014.

[15] P. Du, A. Samat, B. Waske, S. Liu, and Z. Li, "Random Forest and Rotation Forest for fully polarized SAR image classification using polarimetric and spatial features," *Isprs J. Photogramm. & Remote Sens*, vol. 105, pp. 38-53, Jul. 2015.

[16] Berthod, B.; Kato, Z.; Yu, S.; Zerubia, J. Bayesian image classification using Markov random fields. *Image. Vision. Comput*. 1996, 14, 285-295, DOI: https://doi.org/10.1016/0262-8856(95)01072-6

[17] T. Geldsetzer, J.J. Yackel, "Sea ice type and open water discrimination using dual co-polarized C-band SAR," *Remote Sens.*, vol. 35, no. 1, pp.73-84, 2009.

[18] M. Marbouti, O. Antropov, J. Praks, P. Eriksson, V. Arabzadeh, E. Rinne, M. Leppäranta, "TanDEM-X multiparametric data features in sea ice classification over the Baltic Sea," *Remote Sens.*, submitted, 2017.